Synthesis and Photoinitiating Activity Study of Polymeric Photoinitiators Bearing BP Moiety Based on Hyperbranched Poly(ester-amine) via Thiol-ene Click Reaction

Han Xie, Lihua Hu, Wenfang Shi

CAS Key Laboratory of Soft Matter Chemistry, Department of Polymer Science and Engineering, University of Science and Technology of China, Hefei, Anhui 230026, People's Republic of China

ABSTRACT: A series of polymeric photoinitiators (BP-HPEAs) bearing BP moiety based on hyperbranched poly(ester-amine) were synthesized via the thiol-ene click reaction of 3-(4-benzoylphenoxy)propyl 2-mercaptoacetate (BPPM) with acrylated HPEA. BPPM was obtained by the esterification of (4-(3-hydroxypropoxy) phenyl) phenyl methanone (HPPM) with mercaptoacetic acid in the presence of *p*-toluene sulphonic acid as a catalyst. HPEA was prepared through Michael addition of piperazine with tri(hydroxymethyl)propane triacrylate. Their molecular structures were confirmed by the ^{1}H NMR, ^{13}C NMR, and FTIR analysis. The UV–vis spectrum analysis results showed that BP-HPEAs exhibit the stronger n–π^* absorption at $\sim$ 340 nm with over two times higher molar extinction coefficients than BP at the concentration of $1.00 \times 10^{-3} M$. The photoinitiating activity study showed that the maximum photopolymerization rates of 1,6-hexanediol diacrylate initiated by BP-HPEAs in the absence of coinitiator were obtained by two times higher than that by BP in the presence of triethylamine as a coinitiator. Moreover, the excellent miscibility of BP-HPEAs with the commercial bisphenol A epoxy diacrylate was achieved according to the T_s/T_g ratios of over 9.0 from DMTA. © 2011 Wiley Periodicals, Inc. J Appl Polym Sci 123: 1494–1501, 2012

Key words: hyperbranched; initiators; photoinitiating activity; photopolymerization; thiol-ene click reaction

INTRODUCTION

UV curing has been one of the cleanest environment technologies used in protective coatings, printing inks, and adhesives for its low emission of volatile organic compounds and low consumption of energy.[1,2] Photoinitiators that are applied in a small percentage in formulations play a key role in UV curing process as well the properties of end product. However, the commercially supplied conventional photoinitiators with low-molecular weights exhibit some inherent disadvantages, such as odor or migration of photolysis species from cured films.[3,4] Therefore, many researchers in academic and industrial areas are concentrating on the development of polymeric and polymerizable photoinitiators.[5–7] Benzophenone (BP) is a type II free radical photoinitiator and has been widely used in wood, plastic, and paper coatings and inks because of its low cost and high photoinitiating activity in the presence of coinitiators.

Hyperbranched polymers have received extensive attention in recent decades for their unique properties.[8] Frey and Yin[9–12] reported the synthesis and photoinitiating behavior of multifunctional hyperbranched/dendritic polymeric photoinitiators. The thiol-ene click chemistry has aroused great interest for its unique merits,[13,14] such as high yield under moderate reaction conditions,[15] self-initiating,[16,17] and minimal oxygen inhibition[18] in UV curing. Sulfur was reported to be much preferable for preparing photoinitiatiors.[19] And sulfur atom in photoinitiators may lead to obvious red shift in the UV–vis spectra.[20] Moreover, there may undergo photolysis reaction at C—S bond as that in type I aside from H-abstraction reaction,[21] which could greatly enhance the photoinitiating efficiency.[22–24] Yin et al.[25–27] synthesized a series of macroinitiator bearing BP and sulfur. However, little work has been done for preparing hyperbranched polymeric BPs containing both amine and sulfur via thiol-ene click chemistry.

In this work, the polymeric photoinitiators (BP-HPEAs) bearing BP moiety and acrylic double bond at the terminals based on hyperbranched poly(ester-amine) with build-in amine were synthesized via thiol-ene click reaction of 3-(4-benzoylphenoxy)-propyl 2-mercaptoacetate (BPPM) with acrylated HPEA. HPEA was prepared through Michael

addition of piperazine with tri(hydroxymethyl)propane triacrylate. The ^{1}H NMR, ^{13}C NMR, and FTIR spectroscopy were used to characterize the molecular structures. The photoinitiating activity and the compatibility with acrylate oligomers were investigated using photo-DSC and DMTA methods, respectively.

EXPERIMENTAL

Instruments

The FTIR spectra were recorded with a MAGNA-IR 750 spectrometer (Nicolet Instrument Co., USA). The UV–vis spectra were recorded with a SHIMDZU UV2401pc instrument. The ^{1}H NMR spectra were recorded with a DMX-300MHz instrument (Bruker, Switzerland). The number–average molecular weight was determined by a gel permeation chromatography (GPC) equipped with a Waters 1515 pump and 2414 differential refractive index detector (set at 30°C), as well two linear Styragel columns HT3, HT4 at 60°C. DMF was used as an eluent at a flow rate of 1.0 mL min^{-1}.

The photopolymerization rate was monitored in air at 25°C with a differential scanning calorimeter (DSC) equipped a UV spotcure system from TA Instrument (USA). About 2 mg homogeneous formulation was weighted into an aluminum pan. The incident light intensity at the sample pan was measured to be 25 mW cm^{-2} using a UV power meter. The unsaturation conversion (P^f) was calculated by the formula, $P^f = H_t/H_\infty$, where H_t is the heat effect within ts and H_∞ is the heat effect of 100% unsaturation conversion. The DSC curve was normalized by the weight (g) of sample. The polymerization rate was defined as J g^{-1} s^{-1}, namely, the heat of polymerization per second for 1 g samples. For calculating the polymerization rate and H_∞, the value $\Delta H_0 = 86$ J mmol^{-1}, for the heat of polymerization per acrylic unsaturation, was taken.

The tensile storage modulus (E') and tensile loss factors (tan δ) were measured with a Diamond DMA instrument from PE Co. (USA) at a frequency of 10 Hz and heating rate of 10°C min^{-1} in the range of −70–180°C with the sheet of 25.0 mm × 4.0 mm × 1.0 mm.

Materials

Dichloromethane, toluene, triethylamine, p-toluene sulphonic acid (PTSA), sodium hydrate, sodium bicarbonate, piperazine, and mercaptoacetic acid were supplied by Sinopharm Chemical Reagent Co. (China). 1,6-Hexanediol diacrylate (HDDA) and trimethylolpropane triacrylate (TMPTA) were provided by Eternal Chemical Co. (Taiwan). EB605, a standard bisphenol A epoxy diacrylate containing 25 wt % tripropyleneglycol diacrylate, was offered by Cytec

(USA). 4-Hydroxy Benzophenone was purchased from Changzhou Runtec Chemical Co. (China). 3-Chloropropan-1-ol was purchased from Aldrich Chemical Co. (USA). All reagents were of reagent grade and used without further purification.

Synthesis

#### Synthesis of (4-(3-hydroxypropoxy) phenyl) phenyl methanone (HPPM)

4-Hydroxy Benzophenone (20 g and 0.101 mol) was first dissolved in 250 mL of sodium hydroxide aqueous solution (0.404M). Then, 9.49 g 3-chloropropan-1-ol was added dropwise into the above solution at room temperature under stirring and reacted at 100°C for 12 h. The reaction mixture was extracted with dichloromethane (5 × 60 mL). The organic phase was washed again with sodium hydroxide aqueous solution (5 wt %) (3 × 50 mL) and then dried over anhydrous MgSO$_4$. After filtration, evaporation using a rotary evaporator, and drying in a vacuum oven overnight at room temperature, the product, (4-(3-hydroxypropoxy) phenyl) phenyl methanone, named HPPM, was obtained as a white solid (16.8 g, yield: 65%).

^{1}H NMR (CDCl$_3$, 300 MHz): δ = 7.86–6.98 (m, 9H; aromatic), 4.21 (t, 2H; Ar—O—CH_2—), 3.89 (t, 2H; —CH_2—OH), 3.65 (s, 1H; —OH), 2.09 (m, 2H; —CH_2—CH$_2$—OH); ^{13}C NMR (CDCl$_3$, 75 MHz): δ = 195.72 (C=O), 162.57, 138.25, 132.62, 131.97, 130.16, 129.75, 128.23, and 114.05 (aromatic), 65.57 (Ar—O—CH_2—), 59.83(—CH_2—OH), 31.91(—CH_2—CH$_2$—OH); FTIR (KBr, cm^{-1}): 3282 (—OH), 1653 (C=O), 1599 (C=C of benzene of BP moiety), and 1115 (C—O—C).

Synthesis of 3-(4-benzoylphenoxy) propyl 2-mercaptoacetate (BPPM)

HPPM (10.0 g and 0.0391 mol), mercaptoacetic acid (3.77 g and 0.0410 mol), and a catalyst-amount of PTSA (0.413 g and 3.0 wt %) were dissolved in 120 mL of toluene and reacted with stirring under refluxing in N$_2$ atmosphere until no water was formed. The reactant was evaporated to remove toluene with a rotary evaporator, then dissolved in dichloromethane, and further washed with saturated NaHCO$_3$ aqueous solution (3 × 50 mL). The organic phase was dried over anhydrous MgSO$_4$. After filtration and removal of dichloromethane by evaporation, the resultant product was further purified by silica gel column chromatography using dichloromethane/petroleum ether as eluents. After the removal of the solvents, the final product 3-(4-benzoylphenoxy) propyl 2-mercaptoacetate, named BPPM, was obtained as a viscous liquid (10.9 g, yield: 85%).

^{1}H NMR (CDCl$_3$, 300 MHz): δ = 7.86–6.98 (m, 9H; aromatic), 4.21 (t, 2H; Ar—O—CH_2—), 4.15 (t, 2H;
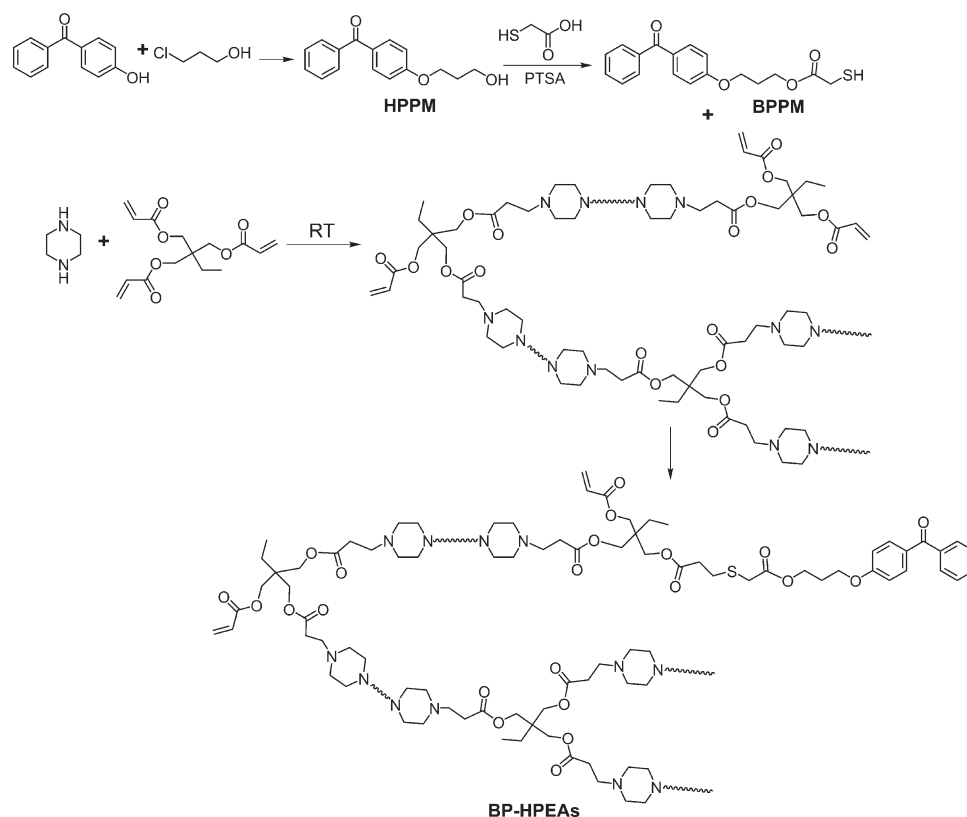
Scheme 1 Schematic illustration for the preparation of derivatives HPPM and BPPM of BP and BP-HPEAs.

—COO—CH$_2$—), 3.26 (d, 2H; —CH$_2$—SH), 2.20 (t, 1H; —CH$_2$—SH), 2.09 (m, 2H; Ar—O—CH$_2$—CH$_2$—); ^{13}C NMR (CDCl$_3$, 75 MHz): δ = 195.56 (C=O of BP moiety), 170.86 (—COO—), 162.33, 138.23, 132.60, 131.96, 130.34, 129.75, 128.23 and 114.02 (aromatic), 64.41 (Ar—O—CH$_2$—), 62.30 (—COOCH$_2$—), 28.42 (Ar—O—CH$_2$—CH$_2$—), 26.48 (—CH$_2$—SH); FTIR (KBr, cm^{-1}): 2568 (—SH), 1736 (C=O of saturated ester moiety), 1653 (C=O of BP moiety), 1599 (C=C of benzene of BP moiety), and 1115 (C—O—C).

Synthesis of BP-terminated hyperbranched poly(ester-amine)s (BP-HPEAs)

Acrylated hyperbranched poly(ester-amine) (HPEA) terminated by double bond and containing build-in amine was synthesized according to the literature.[28] About 7.25 g (24.5 mmol) TMPTA, and 1.485 g (17.25 mmol) piperazine were, respectively, dissolved in 75 mL of THF. The TMPTA solution was added dropwise into the piperazine solution in ice-water bath within 1 h and then reacted for 10 h under stirring at room temperature.

For preparing the BP-terminated HPEA, 2.50 g (7.60 mmol) BPPM in 50 mL of THF was added to the above reactant and reacted until the peak at 2568 cm^{-1} for thiol in the FTIR spectrum disappeared. Then, the reaction mixture was poured into cool ethyl ether. The upper ethyl ether solution was dis-

carded, obtaining the final product, BP-terminated HPEA, named BP-HPEA-1, as a viscous liquid (9.05 g, yield: 80.6%)

For preparing the BP-HPEAs with different numbers of terminal BP moiety, 3.75 g (11.4 mmol) and 5.00 g (15.2 mmol) BPPM were used to react with HPEA, obtaining the products, named BP-HPEA-2 (10.25 g, yield: 82.1%) and BP-HPEA-3 (11.4 g, yield: 83.0%), respectively.

^{1}H NMR (CDCl$_3$, 300 MHz): δ = 7.86–6.95 (aromatic), 6.43–5.84 (CH$_2$=CH—COO—), 4.47–4.02 (—COOCH$_2$— and Ar—O—CH$_2$—), 3.24–3.22 (—S—CH$_2$—COO—), 2.91–2.48 (Ar—O—CH$_2$—CH$_2$—, —S—CH$_2$—CH$_2$—COO— and (—CH$_2$CH$_2$)$_2$—N—CH$_2$CH$_2$—COO—), 1.57–1.45 (—CH$_2$—CH$_3$), 0.95–0.87 (—CH$_2$—CH$_3$); FTIR (KBr, cm^{-1}): 1732 (C=O of saturated ester moiety), 1651 (C=O of BP moiety), 1599 (C=C of benzene of BP moiety), 1115 (C—O—C), and 810 (C—H of CH$_2$=CH—).

The number–average molecular weight (M_n) and its polydispersity index (PDI) (M_w/M_n) measured with GPC were in agreement with the literature reported by Tang.[28]

UV curing

The synthesized BP-HPEA was blended with EB605 under vigorously stirring until a homogenous viscous solution was formed, then poured into a PTFE
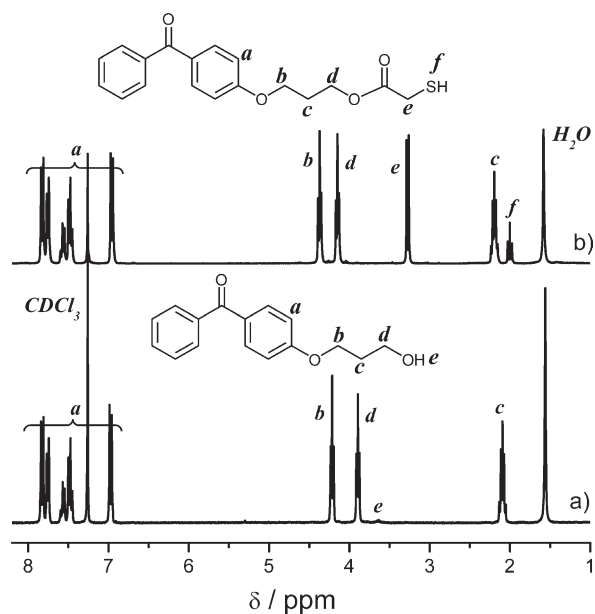
Figure 1 ^{1}H NMR spectra recorded for (a) HPPM and (b) BPPM in CDCl$_3$.

RESULTS AND DISCUSSION

Synthesis and characterization

BPPM containing both thiol group and BP moiety was synthesized via the esterification of HPPM with mercaptoacetic acid in the presence of PTSA. The addition reaction was carried out between TMPTA and piperazine to obtain the acrylated HPEA, which was further terminated by BPPM via thiol-ene click chemistry. As a result, the BP-terminated HPEA (BP-HPEA) with build-in amine and bearing BP moiety and double bond at the terminals was obtained. The
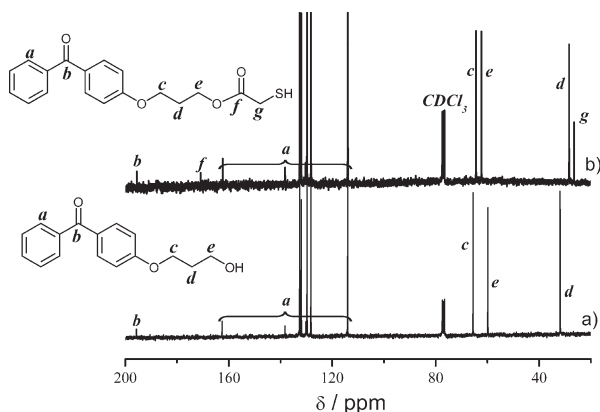

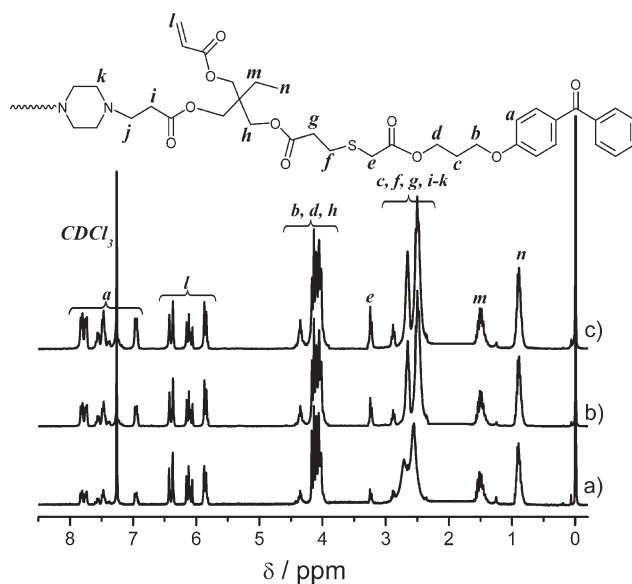**Figure 2** ^{13}C NMR spectra recorded for (a) HPPM and (b) BPPM in CDCl$_3$.

Figure 3 ^{1}H NMR spectra recorded for (a) BP-HPEA-1, (b) BP-HPEA-2, and (c) BP-HPEA-3 in CDCl$_3$.

mold, and exposed to a medium pressure mercury lamp (2 kW, Fusion UV systems, USA) in air. The distance of sample from the UV lamp was set as 15 cm.

thiol-ene click reaction was effectively catalyzed by the build-in amine in the HPEA chain. The synthesis route for BP-HPEA is shown in Scheme 1.

^{1}H NMR and ^{13}C NMR spectra of HPPM and BPPM are, respectively, shown in Figures 1 and 2. The resonance peak at 3.89 ppm in the ^{1}H NMR spectrum is attributed to the protons of methylene next to the terminal hydroxyl group of HPPM and shifts to 4.15 ppm in the ^{1}H NMR spectrum of BPPM, indicating that HPPM has been successfully esterified. Whereas a new resonance peak at 170.86 ppm in ^{13}C NMR spectrum of BPPM attributed to the carbon atom of carbonyl group of ester bond appears, which confirm the existence of ester moiety in BPPM.

Moreover, as the esterification was completed, the absorption peak at 3282 cm^{-1} in the FTIR spectrum of BPPM disappeared, as shown in Figure 4. And the characteristic peaks at 2568 cm^{-1} and 1736 cm^{-1} assigned to the thiol and carbonyl group of ester moiety, respectively, are obviously observed, indicating that BPPM has been successfully obtained. From Figure 4, the absorption peak at 2568 cm^{-1} in the FTIR spectrum of BP-HPEA completely disappeared. This demonstrates that the S—H bond has completely consumed in the addition reaction with HPEA. Whereas, the appearance of characteristic peaks at 1651 cm^{-1}, 1599 cm^{-1}, and 810 cm^{-1} in the FTIR spectrum of BP-HPEA indicates the existence of BP moiety and acrylic double bond in the final product, respectively.

The ^{1}H NMR spectra of BP-HPEAs are similar to each other, but possess different intensity of the characteristic peaks, as shown in Figure 3. The integral ratios of signal peaks for the protons of benzene
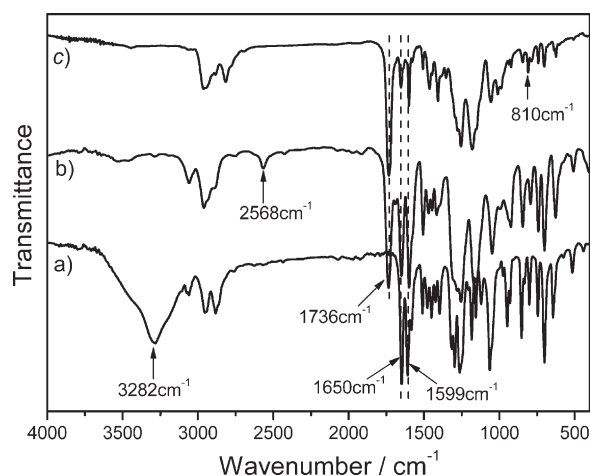
Figure 4 FTIR spectra recorded for (a) HPPM, (b) BPPM, and (c) BP-HPEA-3.

TABLE I
UV–Vis Absorption Wavelengths and Molar Extinction Coefficients of BP and BP-HPEAs in Dichloromethane

Concentration (in terms of BP moiety)	Photoinitiators	λ (nm)	ε (L mol^{-1} cm^{-1})
$1.00 \times 10^{-3}M$	BP	338	1.60×10^2
	BP-HPEA-1	338	3.95×10^2
	BP-HPEA-2	338	4.17×10^2
	BP-HPEA-3	338	4.50×10^2
$1.00 \times 10^{-5}M$	BP	252	2.19×10^4
	BP-HPEA-1	280	1.56×10^4
	BP-HPEA-2	280	1.60×10^4
	BP-HPEA-3	280	1.54×10^4

of BP moiety to that for the protons of acrylic double bond were calculated to be about 0.62 for BP-HPEA-1, 0.93 for BP-HPEA-2, and 1.34 for BP-HPEA-3, indicating that the terminal BP moiety content increases from BP-HPEA-1 to BP-HPEA-3 with increasing BPPM content in the thiol-ene click reaction.
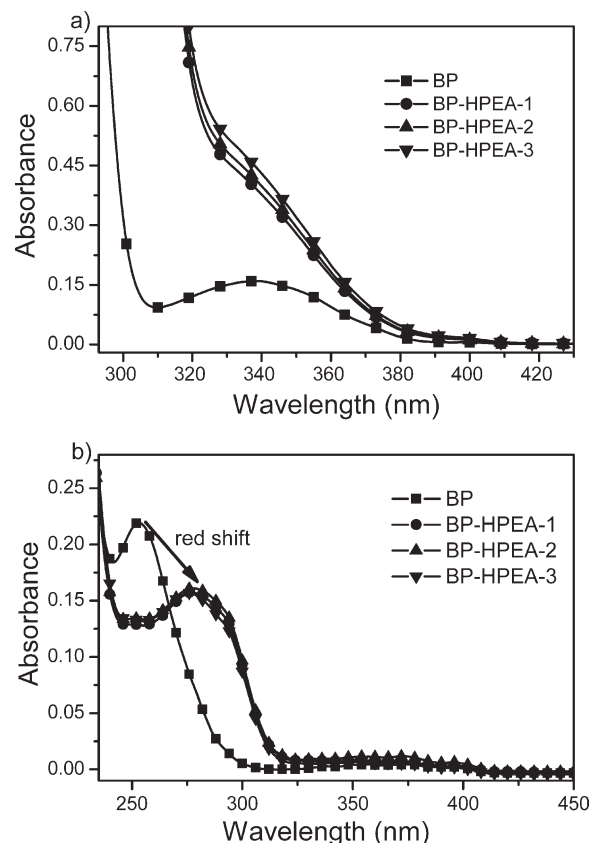
UV–vis absorption spectrum

The UV–vis absorption spectra were investigated at two concentrations of $1.00 \times 10^{-3}M$ and $1.00 \times 10^{-5}M$ of BP-HPEAs in dichloromethane for the comparison with BP, as shown in Figure 5. The absorption of BP in the region of 250–300 nm belongs to the main benzenoid π–π* type transitions, whereas the n–π* type transitions are usually located from 300 to 350 nm due to the spin forbidden transition.[29] Therefore, the molar extinction coefficient of n–π* transitions is considerably weaker than that of

Figure 5 UV–vis absorption spectra recorded for BP and BP-HPEAs with the concentration of (a) $1.00 \times 10^{-3}M$ and (b) $1.00 \times 10^{-5}M$ in CH$_2$Cl$_2$ solution at room temperature.
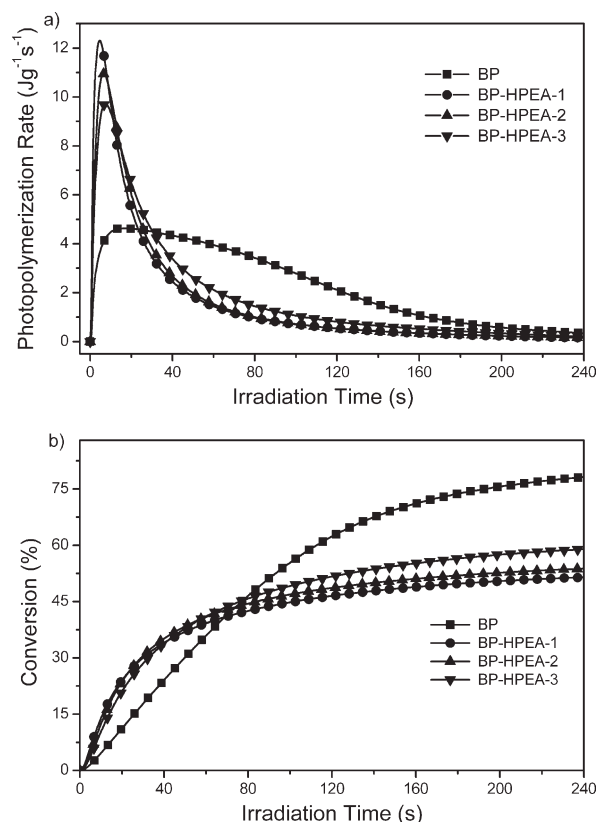

Figure 6 (a) Photo-DSC exotherms and (b) unsaturation conversion curves for the polymerization of HDDA initiated by BP and BP-HPEAs.

TABLE II
Photopolymerization Rate at Peak Maximum (R_p^{max}), the Corresponding Time Spent to Reach R_p^{max} (t^{max}) and Final Unsaturation Conversion (P^f) for the Polymerization of HDDA Initiated by BP and BP-HPEAs

	Formulation composition (wt %)								
Sample	BP-HPEA-1	BP-HPEA-2	BP-HPEA-3	BP	Et₃N	BP moiety	R_p^{max} (J g⁻¹ s⁻¹)	t^{max} (s)	P^f (%)
HD/BP	–	–	–	3.0	3.0	3.0	4.63	17.83	80.7
HD/HPEA-1	24.4	–	–	–	–	3.0	12.31	4.63	52.8
HD/HPEA-2	–	18.1	–	–	–	3.0	10.95	6.63	55.2
HD/HPEA-3	–	–	15.0	–	–	3.0	9.72	7.23	60.5

π–π* type transitions. The UV–vis absorption wavelengths and molar extinction coefficients of BP and BP-HPEAs in dichloromethane are listed in Table I. It can be found that the sulfur-containing BP-HPEAs exhibit much stronger n–π* absorption with high molar extinction coefficients and significant red shift π–π* maximal absorption with the little lower molar extinction coefficients compared to BP. The existence of thioether moiety in BP-HPEAs results in the obvious red shift of their main absorption maximum from ∼ 252 nm of BP to ∼ 280 nm due to increased electron donation via the sulfur atom,[30,31] which may account for their increased photochemical activity during the photopolymerization process.
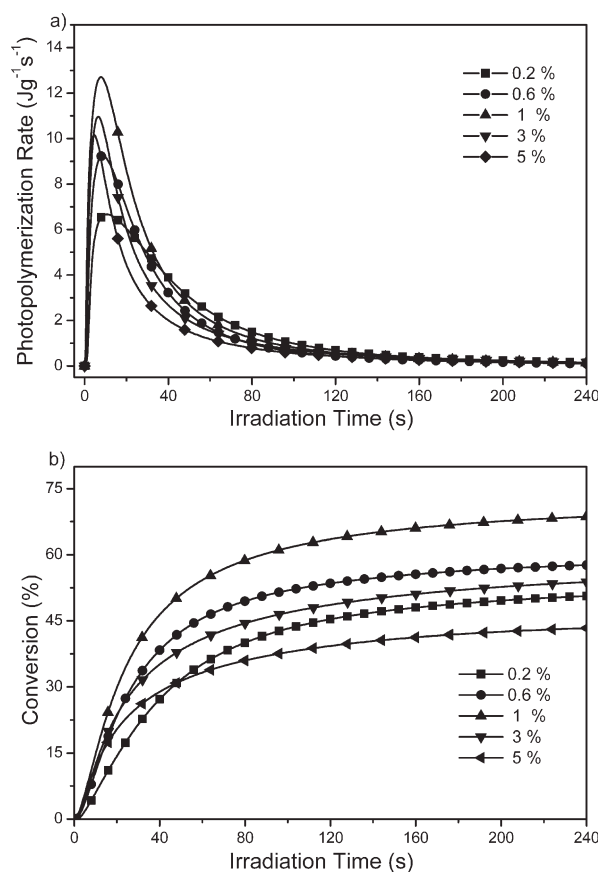

Figure 7 (a) Photo-DSC exotherms and (b) unsaturation conversion curves for the polymerization of HDDA initiated by BP-HPEA-2 in different concentration.

Photoinitiating behavior analysis by photo-DSC

In our work, the photoinitiating activity of synthesized BP-HPEAs was investigated using photo-DSC method by initiating the polymerization of HDDA in comparison with BP at the same BP moiety content. As well known, in the presence of hydrogen donors such as amines or alcohols as coinitiators to eliminate the oxygen inhibition effect, the photolysis of BP results in the formation of radicals derived from the ketyl type radical and also other radicals produced from the hydrogen donor. For the BP photoinitiating system, the same amount of triethylamine (3 wt %) as a coinitiator with BP was added, whereas, for the BP-HPEA photoinitiating systems, no coinitiator was present. The photopolymerization rates (R_p^{max}) and final unsaturation conversion (P^f) in the cured films versus irradiation time are shown in Figure 6. The detailed data together with the formulation composition and the time spent to reach the R_p^{max} (t^{max}) are listed in Table II. It can be seen that the photoinitiating activity of BP-HPEAs is greatly enhanced even at the absence of coinitiator compared to that of BP with coinitiator addition. All the R_p^{max}s of HD/HPEAs are twice higher than that of HD/BP. This can be ascribed to the existence of build-in tertiary amine and sulfur atom in the polymeric main chain.[22,23] Arsu and coworkers[24] also synthesized a polymeric BP photoinitiator, which showed much higher photoinitiating efficiency than BP. However, the final unsaturation conversion in

TABLE III
Photopolymerization Rate at Peak Maximum R_p^{max}), the Corresponding Time Spent to Reach R_p^{max} (t^{max}) and Final Unsaturation Conversion (P^f) for the Polymerization of HDDA Initiated by BP-HPEA-2

	Formulation composition (wt %)				
Sample	BP-HPEA-2	BP moiety	$R_{p_1}^{max}$ (J g⁻¹ s⁻¹)	t^{max} (s)	P^f (%)
HD/HPEA-2/0.2	1.2	0.2	6.67	10.78	51.8
HD/HPEA-2/0.6	3.6	0.6	9.24	8.48	58.5
HD/HPEA-2/1.0	6.0	1.0	12.71	7.83	69.7
HD/HPEA-2/3.0	18.1	3.0	10.95	6.63	55.2
HD/HPEA-2/5.0	30.2	5.0	10.16	4.63	44.3

TABLE IV
DMTA Results of UV-Cured Films Initiated by BP and BP-HPEAs

	Formulation composition (wt %)			Property			
Sample	EB605	Photoinitiators	BP moiety	T_s (°C)	T_g (°C)	T_s/T_g	V_e (mmol cm^{-3})
EB/BP	94.00	3.00 BP/Et$_3$N	3.00	26.3	55.2	0.912	5.81
EB/HPEA-1	91.85	8.15 BP-HPEA-1	1.00	31.2	62.7	0.906	6.59
EB/HPEA-2	93.96	6.04 BP-HPEA-2	1.00	33.5	63.8	0.91	7.05
EB/HPEA-3	95.00	5.00 BP-HPEA-3	1.00	34.8	66.6	0.906	6.57

the UV-cured film initiated by BP is much higher than that by BP-HPEAs. This can be explained by the fact that an efficient UV curable formulation usually previously reaches to the gel point earlier due to the accelerated polymerization rate at the beginning, resulting in the difficulty in diffusion of the formed macromolecular radicals from the microgel network to take further polymerization.

From Figure 6, the R_p^{max} decreases with increasing molecular weight of BP-HPEA at the same BP moiety content. This is supposed to explain as the fact that the increase of molecular weight of BP-HPEA results in the sharp increase of viscosity of the resin, which greatly affect the photopolymerization rate. Contrarily, the P^f increases with increasing molecular weight BP-HPEA as a result of lower viscosity as described earlier.

BP-HPEA-2 was chosen to investigate the effect of BP-HPEA content in the formulation on the photopolymerization kinetic, as shown in Figure 7 and Table III. The photopolymerization rate increases with increasing the BP moiety content until 1.0% and then decreases as BP moiety content further increases. The "autoretarding" phenomenon in photopolymerization behavior initiating by BP has also been observed by other authors.[32] This can be explained that on one hand, the BP moiety in the ground state absorbs UV light in the region of $n-\pi^*$ transition and then act as an "autoretardant"; on the

other hand, some radicals formed in the photolysis of BP will combine with polymer radicals and prevent photopolymerization further. Therefore, BP can be applied as an efficient type II free radical photoinitiator. However, BP also screens the UV light and act as an "autoretardant" when the BP moiety present in a large amount in free radical curing systems. The unsaturation conversion in the UV-cured films shows the same trend with the photopolymerization rates.

Compatibility analysis with UV curable oligomers by DMTA

For investigating the compatibility of BP-HPEAs with UV curable oligomers, a commercial epoxy acrylate resin containing 25 wt % TPGDA (EB605) was used. Therefore, a series of formulations, named EB/BP, EB/HPEA-1, EB/HPEA-2, and EB/HPEA-3, are prepared, as listed in Table IV. And DMTA was used to measure the tensile storage modulus (E') and tensile loss factors (tan δ) of cured EB605 films initiated by BP-HPEAs.

As well known, the peak temperature of a loss factor (tan δ) is defined as the glass transition temperature (T_g); the softening point (T_s) is the extrapolated onset of the drop of log storage modulus (E'). The T_s/T_g ratio indicates the width of the (tan δ) peak. It is well known that the higher the T_s/T_g ratio is, the more homogenous materials are obtained. E' provides the useful information regarding the degree of cured and crosslinking density. The relationship between the rubbery plateau modulus and crosslink density is as follows:

$$V_e = \frac{E'}{3RT}$$

where V_e is the crosslink density, E' is the tensile storage modulus, T is the temperature in Kelvin, and R is the gas constant.

The DMTA curves are shown in Figure 8, and the results are listed in Table IV. It can be seen that the T_s/T_g ratios for all the formulations are above 0.90, indicating that the good miscibility between the polymeric photoinitiators and EB605, and thus homogenous cured films are obtained. Moreover, the
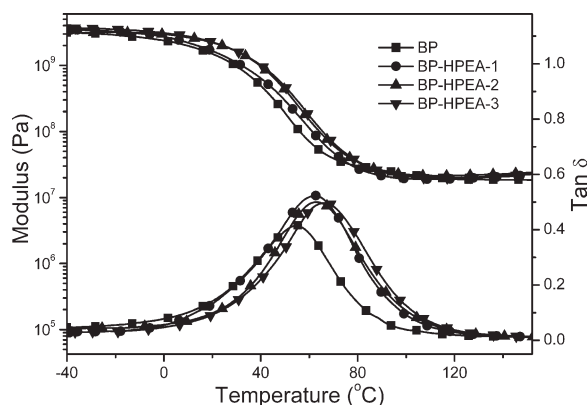

Figure 8 DMTA curves recorded for UV-cured EB605 films initiated by BP and BP-HPEAs at a frequency of 10 Hz and a heating rate of 10°C min^{-1} in the range of −70–180°C.

cured films of EB/HPEAs exhibit higher T_g (over 62°C) and V_e (over 6.5), compared to respective 55.2 and 5.81°C of cured EB/BP film, which could be interpreted that the UV-curable hyperbranched structure of BP-HPEAs results in the increase in crosslink density.

CONCLUSION

In this work, a series of novel hyperbranched polymeric photoinitiators via Michael addition and thiol-ene click reaction were synthesized. ^{1}H NMR and FTIR analyses confirmed the molecular structures. BP-HPEAs possess much stronger absorption at $\sim$ 340 nm and remarkable red shift from $\sim$ 250 to $\sim$ 280 nm when compared with BP in UV–vis spectra. The photo-DSC curves for the polymerization of HDDA initiated by BP-HPEAs exhibited their high photoinitiating efficiency. The good compatibility of BP-HPEAs in the resin was verified by the DMTA.

References

1. Schwalm, R. UV Coatings: Basics, Recent Developments and New Applications; Elsevier: New York, 2007.
2. Zeno, W.; Wicks, J.; Jones, F. N.; Pappas, S. P.; Wicks, D. A. Organic Coatings: Science and Technology, 3rd ed. Wiley-Interscience: New York, 2007.
3. Davidson, R. S.; Dias, A. A.; Illsley, D. J Photochem Photobiol A 1995, 89, 75.
4. Wang, C. Y.; Wei, L.; Lai, G. Q.; Zhong, T. G.; Shen, Y. J. Polym Adv Technol 2010, 21, 72.
5. Yamamoto, Y.; Nakao, W.; Atago, Y.; Ito, K.; Yagci, Y. Eur Polym J 2003, 39, 545.
6. Corrales, T.; Catalina, F.; Peinado, C.; Allen, N. S.; Rufs, A. M.; Bueno, C.; Encinas, M. V. Polymer 2002, 43, 4591.
7. Sarker, A. M.; Sawabe, K.; Strehmel, B.; Kaneko, Y.; Neckers, D. C. Macromolecules 1999, 32, 5203.
8. Gao, C.; Yan, D. Prog Polym Sci 2004, 29, 183.
9. Chen, Y.; Loccufier, J.; Vanmaele, L.; Frey, H. J Mater Chem 2007, 17, 3389.
10. Chen, Y.; Loccufier, J.; Vanmaele, L.; Barriau, E.; Frey, H. Macromol Chem Phys 2007, 208, 1694.
11. Jiang, X. S.; Wang, W. F.; Xu, H. J.; Yin, J. J Photochem Photobiol A 2006, 181, 233.
12. Jiang, X. S.; Xu, H. J.; Yin, J. Polymer 2005, 46, 11079.
13. Dondoni, A. Angew Chem Int Ed 2008, 47, 8995.
14. Hoyle, C. E.; Lowe, A. B.; Bowman, C. N. Chem Soc Rev 2010, 39, 1355.
15. Gress, A.; Völkel, A.; Schlaad, H. Macromolecules 2007, 40, 7928.
16. Cramer, N. B.; Reddy, S. K.; Cole, M.; Hoyle, C.; Bowman, C. N. J Polym Sci Part A: Polym Chem 2004, 42, 5817.
17. Fu, Q.; Liu, J.; Shi, W. Prog Org Coat 2008, 63, 100.
18. O'Brien, A. K.; Cramer, N. B.; Bowman, C. N. J Polym Sci Part A: Polym Chem 2006, 44, 2007.
19. Paczkowski, J.; Kucybala, Z.; Scigalski, F.; Wrzyszczynski, A. J Photochem Photobiol A 2003, 159, 115.
20. Wang, H. Y.; Wei, J.; Jiang, X. S.; Yin, J. J Photochem Photobiol A 2007, 186, 106.
21. Allen, N. S.; Corrales, T.; Edge, M.; Catalina, F.; Blanco-Pina, M.; Green, A. Eur Polym J 1998, 34, 303.
22. Allen, N. S.; Corrales, T.; Edge, M.; Catalina, F.; Blanco-Pina, M.; Green, A. Polymer 1998, 39, 903.
23. Wei, J.; Liu, F. Macromolecules 2009, 42, 5486.
24. Temel, G.; Karaca, N.; Arsu, N. J Polym Sci Part A: Polym Chem 2010, 48, 5306.
25. Wang, H. Y.; Wei, J.; Jiang, X. S.; Yin, J. Polymer 2006, 47, 4967.
26. Wei, J.; Wang, H.; Jiang, X.; Yin, J. Macromolecules 2007, 40, 2344.
27. Wei, J.; Wang, H. Y.; Yin, J. J Polym Sci Part A: Polym Chem 2007, 45, 576.
28. Tang, L. M.; You, H.; Wu, J.; Yu, K.; Tang, X. L. Colloid Surf A 2006, 275, 177.
29. Jauk, S.; Liska, R. Macromol Rapid Commun 2005, 26, 1687.
30. Wrzyszczynski, A.; Bartoszewicz, J.; Hug, G. L.; Marciniak, B.; Paczkowski, J. J Photochem Photobiol A 2003, 155, 253.
31. Matsushima, H.; Hait, S.; Li, Q.; Zhou, H.; Shirai, M.; Hoyle, C. E. Eur Polym J 2010, 46, 1278.
32. Qu, B. J.; Rånby, B. J Appl Polym Sci 1993, 48, 701.